

**The following resources related to this article are available online at [www.sciencemag.org](http://www.sciencemag.org) (this information is current as of September 1, 2009):**

**Updated information and services**, including high-resolution figures, can be found in the online version of this article at:

<http://www.sciencemag.org/cgi/content/full/325/5944/1118>

**Supporting Online Material** can be found at:

<http://www.sciencemag.org/cgi/content/full/325/5944/1118/DC1>

A list of selected additional articles on the Science Web sites **related to this article** can be found at:

<http://www.sciencemag.org/cgi/content/full/325/5944/1118#related-content>

This article **cites 28 articles**, 10 of which can be accessed for free:

<http://www.sciencemag.org/cgi/content/full/325/5944/1118#otherarticles>

This article has been **cited by** 1 articles hosted by HighWire Press; see:

<http://www.sciencemag.org/cgi/content/full/325/5944/1118#otherarticles>

This article appears in the following **subject collections**:

Paleontology

<http://www.sciencemag.org/cgi/collection/paleo>

Information about obtaining **reprints** of this article or about obtaining **permission to reproduce this article** in whole or in part can be found at:

<http://www.sciencemag.org/about/permissions.dtl>

The role of the Quasi-biennial Oscillation (QBO) in the response to solar forcing has been noted in earlier studies (3). A set of experiments with the two WACCM model versions with a prescribed QBO has been carried out, and results from those experiments will be presented in a subsequent paper. However, the results for the climate system response to solar forcing are qualitatively similar to those presented here without the QBO, but the prescribed QBO shows improvements in the stratospheric response compared to observations. Though the solar-forced eastern equatorial SST anomalies shown here are about half the amplitude of those associated with the El Niño–Southern Oscillation, they are relevant for understanding decadal time-scale variability in the Pacific. This response also cannot be used to explain recent global warming because the 11-year solar cycle has not shown a measurable trend over the past 30 years (10).

#### References and Notes

- H. van Loon, G. A. Meehl, J. M. Arblaster, *J. Atmos. Sol. Terr. Phys.* **66**, 1767 (2004).
- H. van Loon, G. A. Meehl, D. J. Shea, *J. Geophys. Res.* **112**, D02108 (2007).
- H. van Loon, K. Labitzke, *Meteorol. Z. (Berlin)* **3**, 259 (1994).
- J. Lean, D. Rind, *Science* **292**, 234 (2001).
- J. Haigh, M. Blackburn, R. Day, *J. Clim.* **18**, 3672 (2005).
- K. Kodera, *Geophys. Res. Lett.* **31**, L24209 (2004).
- H. Gleisner, P. Thejll, *Geophys. Res. Lett.* **30**, 1711 (2003).
- W. B. White, J. Lean, D. R. Cayan, M. D. Dettinger, *J. Geophys. Res.* **102**, 3255 (1997).
- D. Rind, *Science* **296**, 673 (2002).
- J. Lean, G. Rottman, J. Harder, G. Kopp, *Sol. Phys.* **230**, 27 (2005).
- W. B. White, D. R. Cayan, J. Lean, *J. Geophys. Res.* **103**, 21,355 (1998).
- N. Balachandran, D. Rind, P. Lonergan, D. Shindell, *J. Geophys. Res.* **104**, 27,321 (1999).
- D. Shindell, D. Rind, N. Balachandran, J. Lean, J. Lonergan, *Science* **284**, 305 (1999).
- K. Kodera, Y. Kuroda, *J. Geophys. Res.* **107**, 4749 (2002).
- J. Haigh, *Philos. Trans. R. Soc. London A* **361**, 95 (2003).
- K. Matthes, Y. Kuroda, K. Lodera, U. Langematz, *J. Geophys. Res.* **111**, D06108 (2006).
- J. D. Haigh, *Science* **272**, 981 (1996).
- G. A. Meehl, W. M. Washington, T. M. L. Wigley, J. M. Arblaster, A. Dai, *J. Clim.* **16**, 426 (2003).
- G. A. Meehl, J. M. Arblaster, G. Branstator, H. Van Loon, *J. Clim.* **21**, 2883 (2008).
- G. A. Meehl, J. M. Arblaster, *J. Clim.* **22**, 3647 (2009).
- W. B. White, W. B. Z. Liu, *Geophys. Res. Lett.* **35**, L19607 (2008).
- K. Kodera, K. Shibata, *Geophys. Res. Lett.* **33**, L19704 (2006).
- H. van Loon, G. A. Meehl, *J. Atmos. Sol. Terr. Phys.* **70**, 1046 (2008).
- D. T. Shindell *et al.*, *Geophys. Res. Lett.* **33**, L24706 (2006).
- D. Rind, J. Lean, J. Lerner, P. Lonergan, A. Leboisier, *J. Geophys. Res.* **113**, D24103 (2008).
- G. A. Meehl, H. Teng, G. W. Branstator, *Clim. Dyn.* **26**, 549 (2006).
- K. E. Trenberth, J. M. Caron, D. P. Stepaniak, *Clim. Dyn.* **17**, 259 (2001).
- W. B. White, *J. Geophys. Res.* **111**, C09020 (2006).
- Portions of this study were supported by the Office of Science (BER), U.S. Department of Energy, Cooperative Agreement No. DE-FC02-97ER62402, and the NSF. The National Center for Atmospheric Research is sponsored by the NSF.

#### Supporting Online Material

www.sciencemag.org/cgi/content/full/325/5944/1114/DC1

Methods

Figs. S1 to S3

References

27 February 2009; accepted 17 July 2009

10.1126/science.1172872

## Good Genes and Good Luck: Ammonoid Diversity and the End-Permian Mass Extinction

Arnaud Brayard,<sup>1\*</sup> Gilles Escarguel,<sup>2\*</sup> Hugo Bucher,<sup>3,4</sup> Claude Monnet,<sup>3</sup> Thomas Brühwiler,<sup>3</sup> Nicolas Goudemand,<sup>3</sup> Thomas Galfetti,<sup>3</sup> Jean Guex<sup>5</sup>

The end-Permian mass extinction removed more than 80% of marine genera. Ammonoid cephalopods were among the organisms most affected by this crisis. The analysis of a global diversity data set of ammonoid genera covering about 106 million years centered on the Permian-Triassic boundary (PTB) shows that Triassic ammonoids actually reached levels of diversity higher than in the Permian less than 2 million years after the PTB. The data favor a hierarchical rather than logistic model of diversification coupled with a niche incumbency hypothesis. This explosive and nondelayed diversification contrasts with the slow and delayed character of the Triassic biotic recovery as currently illustrated for other, mainly benthic groups such as bivalves and gastropods.

During the Paleozoic and Mesozoic, ammonoids represented an abundant, highly diversified, and geographically widespread group of marine cephalopods. As a major component of open marine biotas, the diversity and evolution of these shelly mollusks closely record the succession of Paleozoic to Mesozoic global changes (1–3). The Permian is characterized by four major, slowly evolving clades of ammonoids

showing a protracted, two-step decline during the Late Permian (Capitanian and Changhsingian extinctions) (4). Only three known ammonoid genera among Ceratitida survived the Permian-Triassic boundary (PTB); with very few exceptions, Triassic ammonoids are usually found to root into a single genus and are therefore interpreted as a monophyletic clade (1, 3, 5, 6). Their extinction selectivity and patterns of recovery have been addressed through changes of morphological diversity (7–9), taxonomic richness, endemism, and biogeographical distribution viewpoints (1, 2). One problem has been a lack of absolute age calibration of evolutionary trends across the PTB. We have used diversity analyses combined with recently published radiometric ages (10) to show that Triassic ammonoids diversified explosively in the first million years after the PTB.

It has usually been assumed that the end-Permian mass extinction affected ecological as-

semblages so deeply that the postcrisis biotic recovery spanned the entire Early Triassic [~5 million years (My) (11)], if not more (12–14). To test this scenario, we constructed a global taxonomic data set at the generic level, from the Late Carboniferous [Kasimovian, 307 million years ago (Ma)] to the Late Triassic (Rhaetian, 201.5 Ma). For each time bin, we considered all documented occurrences of ammonoid genera for each major oceanic sedimentary basin. The resulting data table records the occurrence of 860 genera within 77 basins through 25 successive time bins of unequal duration. Paleozoic ammonoid data are independently derived from the last versions of the Goniatic and Ammon databases (15, 16); Triassic ammonoid data are compiled from various sources (10), with the latest published genera and occurrences added in all cases. Due to distinct taxonomic treatments between the two Paleozoic databases, higher generic richness counts per time bin are obtained from Ammon (Fig. 1), but these differences have no consequence on origination and extinction rate estimates (fig. S1). We thus selected the published Goniatic database for further analyses.

For each time bin, we derived the total (observed + inferred;  $S_{\text{obs}}$ ) number of genera and estimated overall generic richness using Chao2 and Jackknife2 nonparametric indices (10) (Fig. 1 and table S1). Due to the nature of the available data (generic occurrences within basins), the close correspondence between  $S_{\text{obs}}$  and Chao2 and Jackknife2 estimators is strong evidence that most time bins have qualitatively similar structures of observed basin incidences resulting from comparable taxonomical practices and sampling efforts along the analyzed time series. There is no evidence that Triassic time bins contain more genera falsely identified as singletons (i.e., genera spanning only one time bin) than Permian ones. When combined with the

<sup>1</sup>UMR-CNRS 5561 Biogéosciences, Université de Bourgogne, 6 Boulevard Gabriel, F-21000, Dijon, France. <sup>2</sup>UMR-CNRS 5125 PEPS, Université Lyon 1, Campus de la Doua, Bât. Géode, 2 Rue Dubois, F-69622 Villeurbanne Cedex, France. <sup>3</sup>Paläontologisches Institut und Museum, Universität Zürich, Karl-Schmid Strasse 4, CH-8006 Zürich, Switzerland. <sup>4</sup>Department of Earth Sciences, ETH Zürich, Switzerland. <sup>5</sup>Department of Geology and Paleontology, University of Lausanne, l'Anthropole, Lausanne, Switzerland.

\*To whom correspondence should be addressed. E-mail: arnaud.brayard@u-bourgogne.fr (A.B.); gilles.escarguel@univ-lyon1.fr (G.E.)

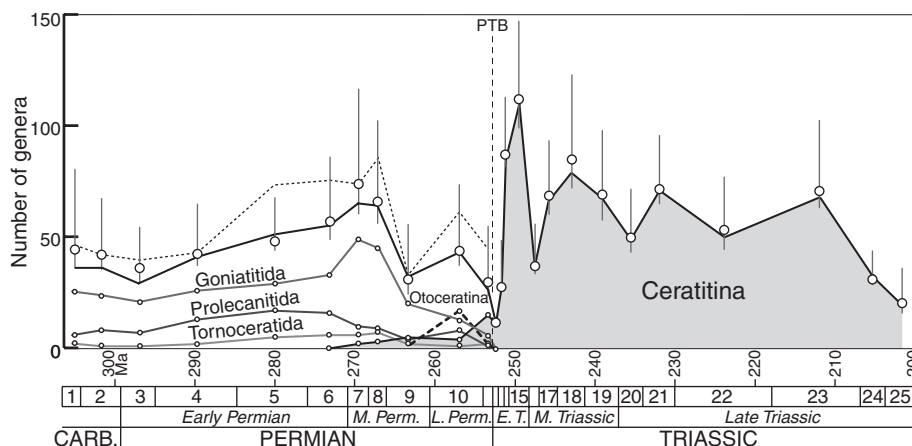


**Fig. 1.** Total generic richness [ $S_{\text{obs}}$ ; black bold line, all ammonoids; gray lines, major ammonoid groups; Permian dotted line, alternate data from Ammon (16)] and mean Chao2 estimate of the overall generic richness with its 95% confidence interval (large circles with vertical bars) (table S1). PTB, Permian-Triassic boundary; 1, Kasimovian; 2, Gzhelian; 3, Asselian; 4, Sakmarian; 5, Artinskian; 6, Kungurian; 7, Roadian; 8, Wordian; 9, Capitanian; 10, Wuchiapingian; unlabeled successive intervals, Changhsingian, Griesbachian, Dienerian, Smithian; 15, Spathian; 16, Early Anisian; 17, Middle Anisian; 18, Late Anisian; 19, Ladinian; 20, Early Carnian; 21, Late Carnian; 22, Early Norian; 23, Middle Norian; 24, Late Norian; 25, Rhaetian. The end-Smithian ammonoid extinction event discussed in the text is not illustrated here due to its short time duration.

lack of statistical dependence between the numbers of sampled basins and singletons (Spearman  $\rho = 0.364$ ,  $P = 0.088$ , not significant), this suggests that time bins with abundant singletons reflect intervals with high generic richness and turnover and are not spurious taxonomical, preservational, and/or sampling artifacts. For this reason, we only describe results based on  $S_{\text{obs}}$ .

The poly-cohort matrix (PCM) (Fig. 2) (17), numbers and rates of generic origination and extinction (Fig. 3 and tables S2 and S3), and phase diagram (fig. S4) show that ammonoid genera smoothly cross the Carboniferous-Permian boundary, in agreement with previous studies of the Carboniferous and Permian (8, 9). This stands in contrast with turnover at the family level (fig. S2). As shown before (4, 8), there is a slight increase in total diversity from the end-Carboniferous onward, culminating in the Middle Permian. Early-Middle Permian diversities are essentially governed by fluctuations in the Goniatitida (Fig. 1). During this time interval, the nonparallelism between the PCM's diagonal (the target assemblage axis) (fig. S5) and pre-nescence and survivorship contour lines (Fig. 2) emphasizes the relatively slow and uncoupled origination and extinction dynamics of Permian ammonoids (Fig. 3). During the Late Permian, temporal diversity patterns are marked by two well-known successive phases of severe extinctions (Capitanian and Changhsingian) (4, 9). This time interval of decreasing morphological diversity (8) corresponds to the progressive decline of Goniatitida and Prolecanitida and to the rise of Ceratitida (Ceratitina and Otoceratitina) (Fig. 1 and fig. S2). Prefiguring the post-PTB diversification dynamics, an increase in diversity observed during the Wuchiapingian stage, between the two major extinction events, resulted mainly from the rapid diversification of Otoceratitina, while Goniatitida experienced a marked diversity decline. This turnover is also well illustrated by the PCM graph and associated cluster analysis (Fig. 2), as well as by the phase diagram (fig. S4).

The Triassic part of the time series consists of four successive diversity oscillations of declining magnitude, probably primarily shaped by global climatic and oceanographic changes (1, 18)

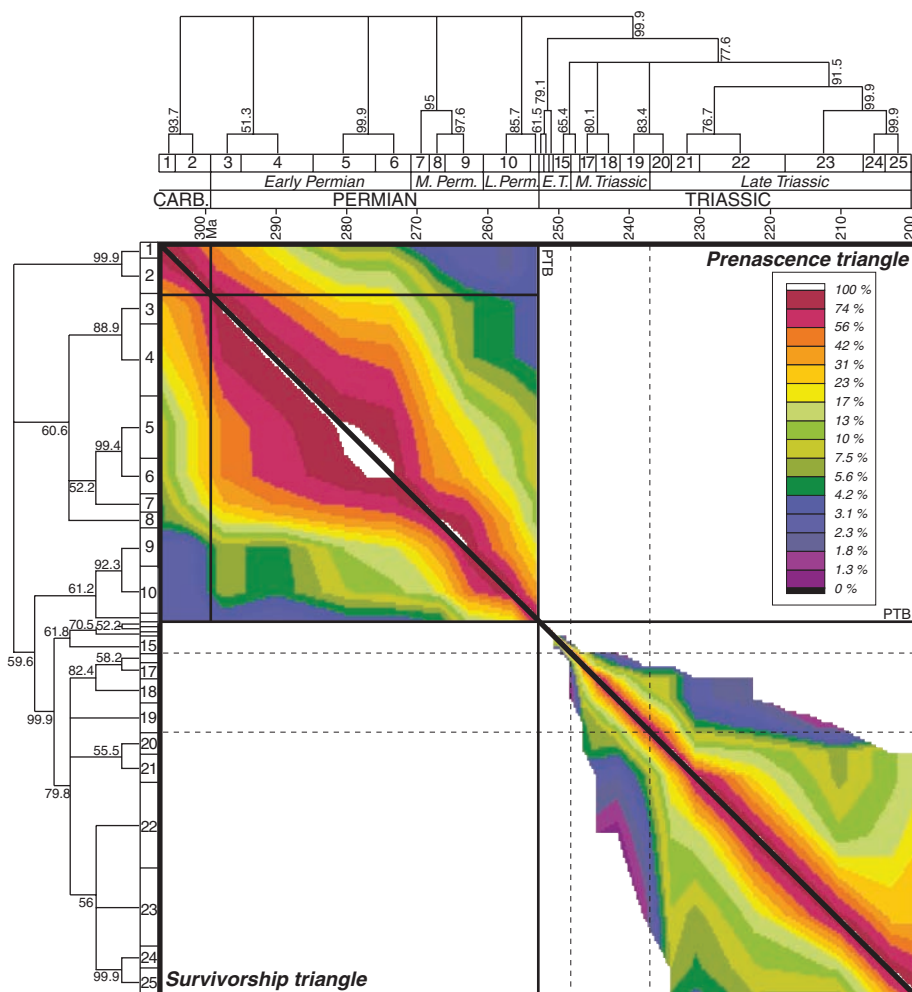


**Fig. 2.** Contour graph of the ammonoid poly-cohort matrix (PCM) (see fig. S5 for details). A poly-cohort is a set of taxa existing during a given time bin; the upper (prenescence) and lower (survivorship) PCM triangles record the origination and extinction dynamics of the target poly-cohort assemblages (PCM diagonal) as the percentage of taxa already or still existing before or after a time span  $\delta t$ , respectively. Associated trees are Neighbor-Joining majority rule consensus topologies (10,000 nonparametric bootstrap replicates; branch lengths not to scale) corresponding to the separate analysis of the origination and extinction dynamics (10); node percentages are estimated bootstrap supports. Same abbreviations as in Fig. 1.

(Figs. 1 and 3). In the first oscillation, during the Smithian—i.e., only 1 to 2 My after the PTB, based on the available radiometric ages and asso-

ciated uncertainties (10, 11)—ammonoid diversity reached values equal to, if not higher than, those for the Permian (~85 sampled genera) and

then were followed by still higher values during the Spathian (~110 genera). This late Early Triassic generic richness is unsurpassed during the Middle and Late Triassic, where diversity oscillated around an average value of ~70 sampled genera per time

bin, close to the Middle Permian maximum. This rapid recovery less than 2 My after a mass extinction is also seen for Early Jurassic ammonoids (19).

The Early Triassic rapid ammonoid diversification diverges from delayed recovery after the

PTB suggested for many benthic groups (e.g., 13). Apparently, recovery rates strongly varied across marine clades, and ammonoids boomed well before the oceanic realm returned to a long-term steady state. Our time-calibrated results indicate that there was a very rapid succession of new families and genera during the Early Triassic (Fig. 2 and figs. S2 and S4). Extreme contraction of survivorship and pre-nascence contour lines is diagnostic of high evolutionary rates, as echoed by the simultaneously high numbers and rates of Early Triassic originations and extinctions (Fig. 3). Ammonoid diversification during the Early Triassic produced more than 200 genera in less than ~5 My and was accompanied by a progressive change from cosmopolitan to latitudinally restricted distributions of genera (1). These changes coincide with the emergence of a clear latitudinal diversity gradient during most of the Smithian and Spathian, which suggests that the sea surface temperature gradient increased during the late Early Triassic (1, 2). This trend was not a gradual, continuous, and smooth one. For instance, ammonoid diversity severely dropped at the Smithian-Spathian boundary (1), coinciding with a major short-term perturbation of the global carbon cycle (11, 18, 20, 21). However, (i) ammonoids already reached a diversity level as high as, if not higher than, in the Permian during the Smithian (Fig. 1), and (ii) as for the end-Permian global event, the end-Smithian disturbances did not markedly delay the long-term Triassic ammonoid diversification.

How did these cephalopods flourish in the presumably unstable and harsh environmental conditions prevailing at that time? The same question applies to conodonts, whose Early Triassic diversity dynamics tend to parallel that of ammonoids (22). The mode(s) of life of ammonoids remains conjectural. These marine organisms may have a pseudoplanktonic juvenile stage (1, 23, 24). Ammonoids are morphologically and taxonomically so diverse that it is likely that they occupied a great variety of niches and exploited various food resources. Their high diversity and abundance suggest that diversified and abundant food resources were already available less than 2 My after the PTB. Consequently, even if Early Triassic trophic webs were possibly less complex than Permian and Middle-Late Triassic ones, they were far from devastated. At least some sizeable, while still unknown, primary production made it possible for these two clades to diversify profusely and rapidly despite short-term fluctuations of environmental conditions such as temperature, pH, and O<sub>2</sub> content of oceanic waters (e.g., 1, 18, 25).

The Early-Middle Triassic transition was again marked by a severe drop in ammonoid diversity. In this case, a fall in global sea level is implicated (26). Middle and Late Triassic generic and family richness remained lower than in the late Early Triassic, close to the Middle Permian maximum but with a few more families (~20 versus ~15 per time bin) (Fig. 1 and fig. S2); richness also appeared less variable, possibly because oceanic geochemical conditions stabilized during that time (11, 20, 21).

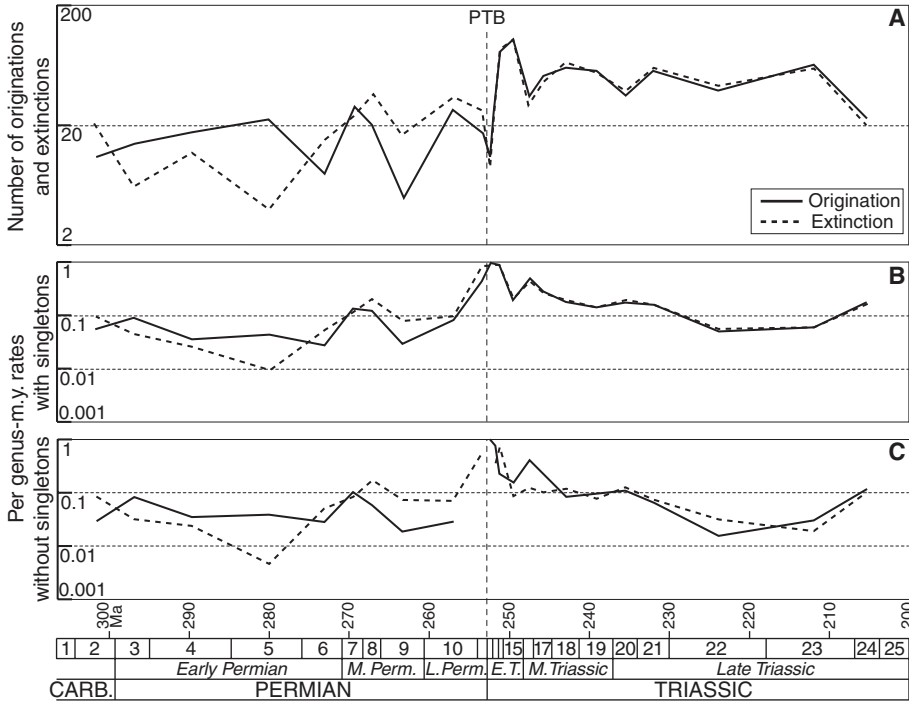


**Fig. 3.** Number of ammonoid genus origination and extinction events (including singletons, i.e., genera spanning only one time bin) (A), and Maurer's (28) per taxon-My origination and extinction rates with (B) and without (C) singletons, calculated for the 25 successive time bins (see table S2 for details). Same abbreviations as in Fig. 1.

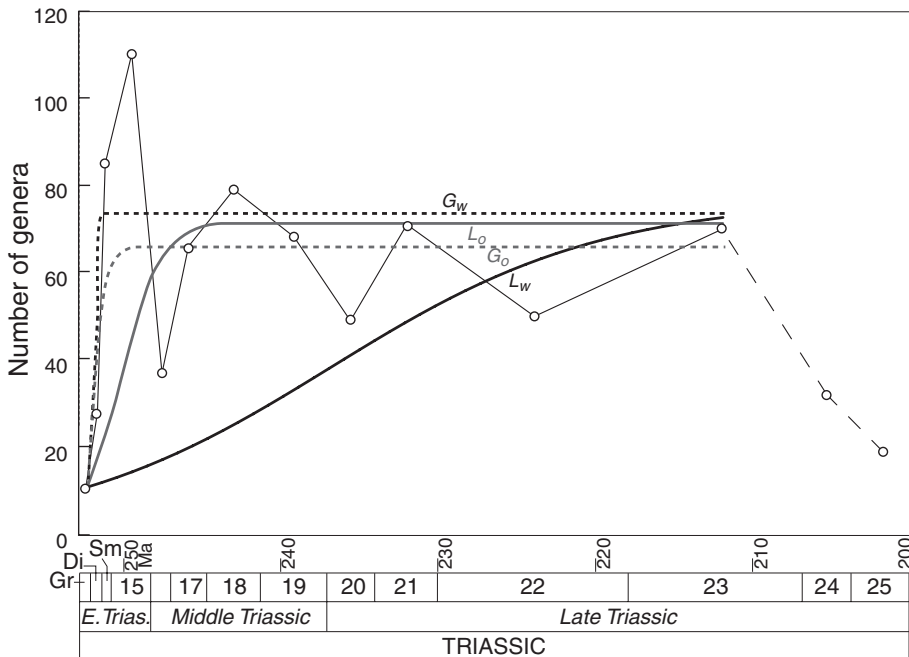


**Fig. 4.** Logistic (L) and hierarchical (G) models of diversification with (w) and without (o) singletons estimated for the Triassic ammonoid data set (tables S4 and S5). Same abbreviations as in Fig. 1. Gr, Griesbachian; Di, Dienerian; Sm, Smithian.

Downloaded from www.sciencemag.org on September 1, 2009

From the early Anisian onward, three successive diversity cycles are evident: Early Anisian–Early Carnian, Early Carnian–Early Norian, and Early Norian–Rhaetian (Figs. 2 and 3). The last cycle ends with a marked diversity decline through the Late Norian and Rhaetian, corresponding to the Triassic–Jurassic mass extinction (19).

Unlike in the Permian, where genera show uncorrelated to weakly correlated origination and extinction dynamics (Fig. 3 and table S2) [linear association between  $\log(N_{Ori}^{t+1}/N_{Ori}^t)$  and  $\log(N_{Ext}^{t+1}/N_{Ext}^t)$ :  $R^2 = 0.060$ ,  $P = 0.56$  for Goniati;  $R^2 = 0.536$ ,  $P = 0.025$  for Ammon], Triassic ammonoids show highly coupled dynamics ( $R^2 = 0.978$ ,  $P = 1.2 \times 10^{-3}$ ) because of the large average proportion of sampled singletons [71% versus 19% (Goniati) to 53% (Ammon) before the PTB]. We investigated the Triassic ammonoid diversity dynamics through diversification models directly derived from the empirical origination and extinction rates (Fig. 4). Based on the overall geometry of the sampled time series (excluding the Late Norian and Rhaetian time bins, which correspond to the end-Triassic mass extinction), we selected two diversity-dependent constrained diversification models: the (evolutionary-based) logistic (27) and (population dynamics-based) hierarchical (28) ones. These models basically differ in the way origination and extinction rates linearly (logistic) or exponentially (hierarchical) relate to taxonomic richness, ultimately leading to a sigmoidal-shaped curve of richness changing through time modeled as a two-parameter logistic function or a three-parameter Gompertz function, respectively. All computations were done based on Maurer's per-taxon per-My origination and extinction rates (28) computed with or without singletons (10). These rates share the same statistical behavior as Foote's estimated per-capita per-My rates (29), with which they highly correlate (table S3). We selected Maurer's rather than Foote's rates because the later cannot be calculated for three of the four Early Triassic time bins, that is, when ammonoids actually recovered (table S2).

Model comparison using evidence ratios calculated from corrected Akaike information criterion values favors the hierarchical diversification model over the logistic one (table S5). Indeed, even if both models converge toward the same steady-state richness values (~70 sampled genera) (Fig. 4), the logistic model clearly fails to capture the Early Triassic nondelayed recovery dynamics, contrary to the hierarchical one. In addition, the empirical (log) richness-rates relationships (table S4) illustrate a possible niche incumbency effect (30). This hypothesis, which predicts that richness and extinction rates are independent, allows the estimate of an average steady-state generic niche saturation level of ~85% under the hierarchical model, compatible with species niche saturation levels previously published for various clades of marine organisms (30).

Numerous Lazarus taxa among benthic and pelagic mollusks reappear during the Smithian (e.g., 6, 31). Coupled with the Triassic ammonoid

nondelayed diversity dynamics evidenced here, this suggests that complex trophic webs based on abundant and diversified primary producers were already functioning less than 2 My after the PTB and opens the possibility that heterotrophic taxa other than ammonoids also rapidly recovered. The end-Smithian global event, possibly linked to a late eruptive phase of the Siberian traps, initiated the conodont demise and corresponds to a major global change in the carbon cycle and climate (8, 18, 20, 21) but did not markedly delay the explosive recovery of Ceratitid ammonoids. This phased scenario for the Triassic biotic recovery accounts well for its generally accepted delayed character, which may reflect still inadequate sampling and time resolution and/or biased diversity estimates due to the lack of sampling standardization in the first million years after the PTB (32, 33). Recoveries obviously show environment- and clade-specific dynamics. Nevertheless, our results indicate that the time duration of the post-PTB recovery is likely overestimated, at least for some marine taxa.

#### References and Notes

1. A. Brayard *et al.*, *Palaeogeogr. Palaeoclim. Palaeoecol.* **239**, 374 (2006).
2. A. Brayard, G. Escarguel, H. Bucher, *Geobios* **40**, 749 (2007).
3. A. J. McGowan, A. B. Smith, *Palaeontology* **50**, 573 (2007).
4. Z. Zhou, B. F. Glenister, W. M. Furnish, C. Spinosa, *Permophiles* **29**, 52 (1996).
5. E. T. Tozer, in *The Ammonoidea*, M. R. House, J. R. Senior, Eds. (The Systematics Association, London, 1981), special vol. 18, pp. 65–100.
6. A. Brayard *et al.*, *Lethaia* **40**, 175 (2007).
7. A. J. McGowan, *Geology* **32**, 665 (2004).
8. L. Villier, D. Korn, *Science* **306**, 264 (2004).
9. W. B. Saunders, E. Greenfest-Allen, D. M. Work, S. V. Nikolaeva, *Paleobiology* **34**, 128 (2008).
10. Data set and methods are available as supporting material on Science Online.
11. T. Galfetti *et al.*, *Earth Planet. Sci. Lett.* **258**, 593 (2007).
12. J. W. Kirchner, A. Weil, *Nature* **404**, 177 (2000).
13. D. H. Erwin, *Proc. Natl. Acad. Sci. U.S.A.* **98**, 5399 (2001).
14. J. Alroy, *Proc. Natl. Acad. Sci. U.S.A.* **105**, 11536 (2008).
15. GONIAT: J. Kullman *et al.*, version 3.5 (March 2007); see [www.goniati.org](http://www.goniati.org).
16. Ammon: D. Korn, A. Ilg, data accessed 05/20/2009; [www.wahre-staerke.com/ammon](http://www.wahre-staerke.com/ammon).
17. G. Escarguel, S. Legendre, B. Sigé, *C. R. Geosci.* **340**, 602 (2008).
18. T. Galfetti *et al.*, *Geology* **35**, 291 (2007).
19. U. Schaltegger, J. Guex, A. Bartolini, B. Schoene, M. Ovtcharova, *Earth Planet. Sci. Lett.* **267**, 266 (2008).
20. T. Galfetti *et al.*, *Palaeogeogr. Palaeoclim. Palaeoecol.* **243**, 394 (2007).
21. J. L. Payne *et al.*, *Science* **305**, 506 (2004).
22. M. J. Orchard, *Palaeogeogr. Palaeoclimatol. Palaeoecol.* **252**, 93 (2007).
23. E. T. Tozer, *Geol. Rundsch.* **71**, 1077 (1982).
24. H. Bucher, N. H. Landman, J. Guex, S. M. Klofak, in *Ammonoid Paleobiology*, N. H. Landman, K. Tanabe, R. A. Davies, Eds. (Plenum, 1996), pp. 407–461.
25. J. L. Payne, L. R. Kump, *Earth Planet. Sci. Lett.* **256**, 264 (2007).
26. A. F. Embry, *Bull. Can. Pet. Geol.* **45**, 415 (1997).
27. J. J. Sepkoski, *Paleobiology* **4**, 223 (1978).
28. B. A. Maurer, *Paleobiology* **15**, 133 (1989).
29. M. Foote, *Paleobiology* **26**, 74 (2000).
30. T. D. Walker, J. W. Valentine, *Am. Nat.* **124**, 887 (1984).
31. M. Hautmann, A. Nützel, *Palaeontology* **48**, 1131 (2005).
32. P. J. Lu, M. Yogo, C. R. Marshall, *Proc. Natl. Acad. Sci. U.S.A.* **103**, 2736 (2006).
33. J. Alroy *et al.*, *Science* **321**, 97 (2008).
34. This article is a contribution from the team Forme, Evolution, Diversité of the UMR-CNRS 5561 Biogéosciences (A.B.), and from the team Adaptation, Morphologie, Environnement of the UMR-CNRS 5125 PEPS (G.E.). This work was supported by the Swiss NSF project 200020-113554 (H.B.). We thank R. Colwell (University of Connecticut, USA) and E. Fara (University of Burgundy, France) for discussion.

#### Supporting Online Material

[www.sciencemag.org/cgi/content/full/325/5944/1118/DC1](http://www.sciencemag.org/cgi/content/full/325/5944/1118/DC1)  
Methods  
SOM Text  
Figs. S1 to S6  
Tables S1 to S5  
References

7 April 2009; accepted 8 July 2009  
10.1126/science.1174638

## Enhancement of Biodiversity and Ecosystem Services by Ecological Restoration: A Meta-Analysis

José M. Rey Benayas,<sup>1,2\*</sup> Adrian C. Newton,<sup>3</sup> Anita Diaz,<sup>3</sup> James M. Bullock<sup>4</sup>

Ecological restoration is widely used to reverse the environmental degradation caused by human activities. However, the effectiveness of restoration actions in increasing provision of both biodiversity and ecosystem services has not been evaluated systematically. A meta-analysis of 89 restoration assessments in a wide range of ecosystem types across the globe indicates that ecological restoration increased provision of biodiversity and ecosystem services by 44 and 25%, respectively. However, values of both remained lower in restored versus intact reference ecosystems. Increases in biodiversity and ecosystem service measures after restoration were positively correlated. Results indicate that restoration actions focused on enhancing biodiversity should support increased provision of ecosystem services, particularly in tropical terrestrial biomes.

**E**cological restoration involves assisting the recovery of an ecosystem that has been degraded, damaged, or destroyed, typically as a result of human activities (1). Restoration

actions are increasingly being implemented throughout the world (2), supported by global policy commitments such as the Convention on Biological Diversity [article 8(f), (3)]. A major